

Universality of an improved photosynthesis prediction model based on PSO-SVM at all growth stages of tomato

Li Ting^{1,3}, Ji Yuhan¹, Zhang Man^{1*}, Sha Sha², Li Minzan¹

(1. Key Laboratory of Modern Precision Agriculture System Integration Research, Ministry of Education, China Agricultural University, Beijing 100083, China; 2. Key Laboratory of Agricultural Information Acquisition Technology, Ministry of Agriculture, China Agriculture University, Beijing 100083, China; 3. Beijing Research Institute of Uranium Geology, Beijing 100029, China)

Abstract: CO₂ concentration is an environmental factor affecting photosynthesis and consequently the yield and quality of tomatoes. In this study, a photosynthesis prediction model for the entire growth stage of tomatoes was constructed to elevate CO₂ level on the basis of crop requirements and to evaluate the effect of CO₂ elevation on leaf photosynthesis. The effect of CO₂ enrichment on tomato photosynthesis was investigated using two CO₂ enrichment treatments at the entire growth stage. A wireless sensor network-based environmental monitoring system was used for the real-time monitoring of environmental factors, and the LI-6400XT portable photosynthesis system was used to measure the net photosynthetic rate of tomato leaf. As input variables for the model, environmental factors were uniformly preprocessed using independent component analysis. Moreover, the photosynthesis prediction model for the entire growth stage was established on the basis of the support vector machine (SVM) model. Improved particle swarm optimization (PSO) was also used to search for the best parameters *c* and *g* of SVM. Furthermore, the relationship between CO₂ concentration and photosynthetic rate under varying light intensities was predicted using the established model, which can determine CO₂ saturation points at the various growth stages. The determination coefficients between the simulated and observed data sets for the three growth stages were 0.96, 0.96, and 0.94 with the improved PSO-SVM and 0.89, 0.87, and 0.86 with the original PSO-SVM. The results indicate that the improved PSO-SVM exhibits a high prediction accuracy. The study provides a basis for the precise regulation of CO₂ enrichment in greenhouses.

Keywords: photosynthesis, greenhouse, tomato, CO₂ enrichment, photosynthesis prediction model, wireless sensor network, environmental monitoring system

DOI: 10.3965/j.ijabe.20171002.2580

Citation: Li T, Ji Y H, Zhang M, Sha S, Li M Z. Universality of an improved photosynthesis prediction model based on PSO-SVM at all growth stages of tomato. *Int J Agric & Biol Eng*, 2017; 10(2): 63–73.

1 Introduction

Solar greenhouse, which is an intelligent production

Received date: 2016-05-17 **Accepted date:** 2016-11-09

Biographies: **Li Ting**, Master, research interest: agricultural informatization, Email: 15201423238@163.com; **Ji Yuhan**, Master, research interest: agricultural informatization, Email: jyh1009845844@163.com; **Sha Sha**, Master, research interest: agricultural informatization, Email: shashaok2010@163.com; **Li Minzan**, PhD, Professor, research interest: precision agriculture, Email: limz@cau.edu.cn.

***Corresponding author: Zhang Man**, PhD, Professor, research interest: precision agriculture. Mailing address: P.O.Box 125, Qinghua East Road, Haidian District, China Agricultural University, Beijing 100083, China. Tel: +86-10-62737188, Email: cauzm@cau.edu.cn.

system, is a trend in the development of facility agriculture. The major crops planted in greenhouses are high-value crops such as leafy vegetables, fruit vegetables, and flowering plants^[1]. Monitoring and control of greenhouse conditions are highly important to provide a growth-conducive environment for these crops. Real-time, convenient, and efficient acquisition of environmental parameters is an important foundation to manage greenhouse conditions.

Wireless sensor network (WSN) is a new technology of information acquisition that has been widely used in agriculture, especially in greenhouses^[2,3]. Mancuso and Bustaffa^[4] developed a knowledge-based decision support system based on WSN. This system measures

the microclimate of a tomato crop to acquire detailed information necessary for the development of a novel decision support system that will help farmers improve crop quality. Srbínovska et al.^[5] designed a practical and low-cost WSN technology-based greenhouse monitoring system for key environmental parameters, such as the temperature, humidity, and illumination. Hwang et al.^[6] also proposed a growth management system to improve productivity by maintaining an optimized environment for crop growth; this system not only can reduce production cost but also conveniently control various greenhouse parameters, such as illumination, temperature, electrical conductivity, pH, and CO₂ concentration. Rapid acquisition of information via WSN provides great convenience in greenhouse management and in conducting research on the influence of environmental factors on greenhouse crops.

In greenhouse crop production, environmental factors such as CO₂ concentration, light intensity, and temperature are highly important for crop growth. CO₂ concentration affects photosynthesis, and CO₂ is one of main raw material for crop growing. Studies have shown that biomass increases by approximately 50% in C3 plants^[7] and 12% in C4 plants^[8] under CO₂ enrichment conditions. In addition, elevated CO₂ significantly increases photosynthetic rate^[9,10]. However, CO₂ is quite expensive and should be applied very efficiently. Excess CO₂ not only increases input costs but also negatively affects crop growth. Therefore, an appropriate CO₂ management scheme must be developed. Measuring the single-leaf photosynthetic rate and establishing a photosynthesis prediction model are necessary to optimize CO₂ regulation. Wang et al.^[11] established a photosynthetic rate prediction model on the basis of the BP neural network at the late seedling and flowering stages, as well as elucidated the effect of CO₂ concentration on crops at various growth stages. Zhang and Wang^[12] constructed a canopy photosynthesis model of tomato on the basis of simple leaf photosynthesis and investigated the influence of environmental factors (e.g., temperature, CO₂, and moisture). Hu et al.^[13] also proposed an optimal photosynthesis regulation model of tomato seedlings on the basis of the genetic algorithm;

this model can measure light saturation point under certain air temperature and CO₂ concentration but involves manual and limited acquisition of environmental information. Furthermore, these studies built models of crops at a single growth stage and lacked observation on crop photosynthesis at the entire growth stage.

The support vector machine (SVM) model, which is based on statistical learning theory and the principle of structural risk minimization, has been applied in nonlinear regression and data prediction. Wang et al.^[14] presented an SVM regression modeling method and online learning approach for greenhouse environment. In addition, Zai et al.^[15] established an SVM model for the determination of leaf area of sweet pepper, and this model exhibits high prediction accuracy and good practical value. Basing on the obtained characteristic spectra, Zhang et al.^[16] established a fruit sugar SVM prediction model with parameter optimization. These studies provided the basis for the establishment of a photosynthesis prediction model. However, the most important problems encountered in establishing an SVM model lie in the selection of kernel functions and other relevant parameters. Grid search is a common method to choose parameters. However, it suffers from several weaknesses, such as the requirement of a large amount of training data, and the time cost would sharply increase as the searching grids become denser^[17]. Kennedy et al.^[18] proposed the PSO (Particle swarm optimization) algorithm, which is a typical group of intelligent algorithms, and is usually used to determine parameters of SVM model because it is simpler and faster. Xu et al.^[19] established the prediction model of the temperature of blast furnace based on the improved PSO-optimized SVM. Liu et al.^[17] proposed IPSO-SVM model, which could achieve higher recognition accuracy and efficiency for online recognition defects in eddy current testing. However, one drawback of the PSO algorithm is easy to fall into local optimum in the case of few training sample. In order to obtain more accurate results, the PSO algorithm needs to be optimized and improved.

Considering the problems mentioned above, this study aimed to build a photosynthesis prediction model for tomato plants by using the improved PSO-SVM, as

well as to quantify the effects of CO₂ on photosynthetic rate. In this study, the environmental parameters collected by WSN were used as input parameters for the model. The net photosynthetic rate measured using the LI-6400XT photosynthesis system was as the output. To verify the generality, the model was tested by using the dataset obtained from three growth stages (i.e., late seedling, full flowering, and early fruiting stages). This model can be used to determine the precise relationship between CO₂ concentration and photosynthetic rate, as well as serve as a basis for the precision regulation of CO₂ enrichment in greenhouses.

2 Materials and methods

2.1 Architecture of the system

To analyze the effect of CO₂ enrichment on photosynthesis and growth of plant during the entire growth stage, the elevated CO₂ experiment was implemented. During the experiment, the WSN-based environmental monitoring system consisting of sensor nodes, a sink node, and a remote data management platform was used to monitor environmental factors in real time and control CO₂ concentration enrichment. The LI-6400XT portable photosynthesis system (LI-COR Inc., Lincoln, NE, USA) was used to measure the net single-leaf photosynthetic rate of tomato, and the data were transmitted into a remote data management platform. Moreover, PSO-SVM and its improved version were used to establish a photosynthesis prediction model that describes the relationship between CO₂ concentration and photosynthetic rate at the three growth stages. Environmental factors were used as input variables for the models after being processed via independent component analysis (ICA), and the photosynthetic rate served as the output variable. Figure 1 shows the system architecture.

2.2 Experimental design

The experiments were performed from April to June 2015 in a greenhouse at the College of Water Conservancy and Civil Engineering, China Agricultural University. As one of the world’s major greenhouse crops, tomato variety “Zhefen 702” was selected as experimental object. The plants were placed in two

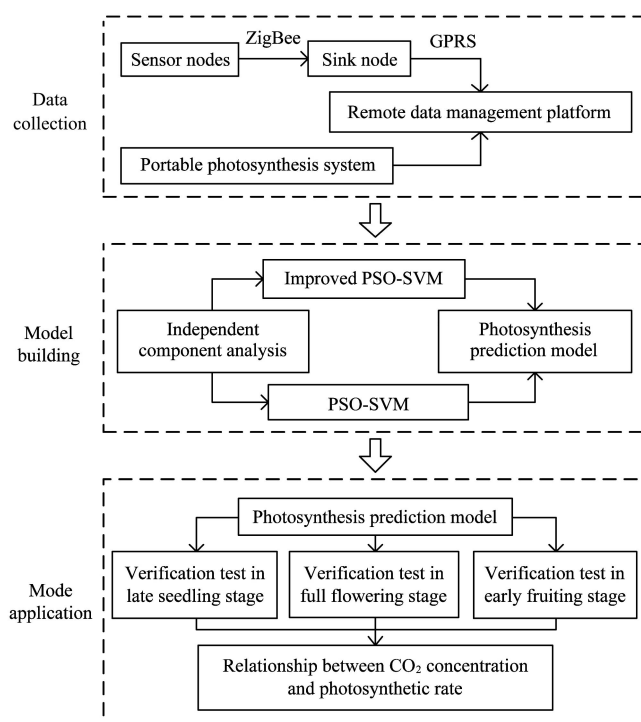


Figure 1 System architecture

cultivation bins with plastic film PEP (2.5 m (length) × 0.6 m (width) × 2.0 m (height)) and then grown under similar conditions (i.e., natural temperature and humidity). The sensor node connected to an electromagnet was used to control the switch of the CO₂ source. The gas was delivered from the cylinders and passed through a pressure-reducing valve for diffusion into the cultivation bin via a white transparent plastic hose, along which 0.2 cm wide holes were placed every 30 cm^[20]. The tomatoes were treated with CO₂ enrichments (1000±50 μmol/mol (C1) and atmospheric CO₂ concentration in greenhouse (CK, approximately 450 μmol/mol)) at the three growth stages.

2.2.1 Collection of environmental information

The environmental information during the entire growth stage of tomato was automatically collected in real time by using the WSN system every 30 min. The system consisted of sensor nodes, a sink node, and a remote data management platform. The sensor nodes, which contain five types of sensors that measure environmental factors, including air temperature and humidity, CO₂ concentration, light intensity, substrate temperature, and moisture, collect and transmit data to the sink node by using the ZigBee protocol. The sink node stores data received from the sensor nodes and sends

these data to the remote data management platform via the general packet radio service module. The remote data management platform exhibits a good man-machine interface and can be used to observe environmental changes, set CO₂ enrichment schedule, and establish a photosynthesis prediction model by combining environmental factors and photosynthetic rate.

2.2.2 Photosynthetic rate measurement

The experiments were divided according to the three growth stages of tomato: late seedling, full flowering, and early fruiting. A similar method in measuring photosynthetic rate was employed at each growth stage.

For each treatment, five tomato plants growing consensus were randomly selected to measure the net photosynthetic rate by using the LI-6400XT portable photosynthesis system. The middle part of fully expands functional leaves which located as the second or third leaf from top to bottom, was measured. To expand the data range, the two-factor interaction experiment was conducted by artificially controlling CO₂ concentration and light intensity. The 6400-01 CO₂-injector system (LI-6400XT portable photosynthesis system accessory) was used to control CO₂ concentration, which was set to 400, 600, 800, 1000, 1300, 1500, and 1700 $\mu\text{mol/mol}$. The 6400-02B red/blue LED light source (light source located on the leaves chamber of LI-6400XT portable photosynthesis system) was used to adjust light intensity, which was set to 1200, 900, 600, and 300 $\mu\text{mol/m}^2\cdot\text{s}$. The natural air temperature and humidity were maintained, i.e., 29.96°C-34.60°C and 15.96%-27.23% in the late seedling stage, 29.54°C-36.23°C and 25.45%-50.93% in the flowering stage, 30.91°C-36.41°C and 17.37%-40.71% in the early fruiting stage, 500 mL/min air flow rate. The measurements were obtained until the photosynthetic rate fluctuation was less than 0.2 $\mu\text{mol/mol}$ for stabilization and the stomatal conductance (Cond), intercellular CO₂ concentration (C_i), and transpiration rate (Tr) were all greater than 0. The CO₂-photosynthetic rate curve was measured aiming to CO₂ saturation points, of which the CO₂ concentration gradient was set to 0, 20, 50, 100, 200, 400, 600, 800, 1000, 1300, 1500, and 1700 $\mu\text{mol/mol}$. To allow the leaves to adapt completely to the artificial environment,

photosynthetic induction was performed under a light intensity of 900 $\mu\text{mol/m}^2\cdot\text{s}$ and other natural environmental parameters prior to measurement; this process took nearly 15 min during summer^[11,21]. To reduce internal system error, a matching operation that was to make equal CO₂ concentration between reference chamber and sample chamber was needed for LI-6400XT when converting a measurement.

2.3 Data analysis methods

The improved PSO-SVM was employed to establish a photosynthesis prediction model by using the data collected from the above-described experiments performed during the entire growth stage of tomato. To render the model accurate, the dataset was processed via ICA and then normalized prior to modeling.

2.3.1 Data preprocessing

The raw dataset measured using the environmental monitoring system had correlation and dependence. Data representing similar sample properties must be removed to avoid extensive calculation and model stability disturbance due to data redundancy. Furthermore, the implicative information of experimental data must be excavated to ensure the quality of the model. ICA is an appropriate method to solve the problems mentioned above prior to modeling^[22].

ICA is also an effective method to decompose blind signals. The original variables can be decomposed into a plurality of mutually independent components (ICs) by calculating the high moments among decomposing components. Equation (1) shows the basic statistical model of ICA:

$$X=AS \quad (1)$$

where, $X=(x_1, x_2, \dots, x_m)$ represents the m -dimension signals; X represents the environmental variables; $S=(s_1, s_2, \dots, s_n)$ represents the mutually independent n -dimension independent component matrix; A is the $m \times n$ hybrid matrix^[23]. The result of ICA is uncertain because both A and S are unknown. A very popular approach in estimating the ICA is the maximum likelihood estimation, where in the cumulative distribution of S is assumed to obey the Sigmoid function. The specific algorithm is shown in the reference section^[24].

In order to eliminate the influence of the different

orders of magnitude and improve SVM training accuracy, the input and output variables of model need to be normalized according to Equation (2). After processing, the data of minimum and maximum values were normalized to $[-1, 1]$.

$$x'_k = 2 \times \frac{(x_k - x_{\min})}{(x_{\max} - x_{\min})} - 1 \quad (2)$$

where, x_{\max} and x_{\min} represent the maximum and minimum values of each variable, respectively.

2.3.2 Support vector machine regression

The classical modeling method cannot meet the modeling requirement because the relationship between the environmental variables and photosynthetic rate is indeterminate and nonlinear. SVM regression is well supported by mathematical theory and exhibits a simple structure, good generalization ability, and nonlinear modeling properties^[14]. Therefore, SVM is a competent method for photosynthesis prediction modelling.

The SVM exhibits a three-layered network structure (Figure 2) and is a machine learning method with multiple inputs and a single output.

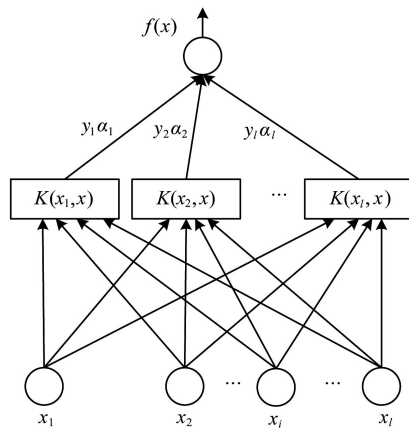


Figure 2 Architecture of SVM

In Figure 2, $\{x_1, x_2, \dots, x_l\}$ and $\{y_1, y_2, \dots, y_l\}$ are respectively the input and output training groups, $K(x_i, x)$ ($i = 1, 2, \dots, l$) is the kernel function, α is the Lagrange multipliers, and $f(x)$ is the decision function. For the data processing, MATLAB 2012a with SVM Toolbox was used. Moreover, random training samples were used as input variables for SVM. Some types of kernel function also exist, such as polynomial kernel function, RBF kernel function, and Sigmoid kernel function. RBF was selected to realize the sample mapping from input space to high-dimensional feature space because RBF can

process nonlinear problems effectively and less interference from the sample outliers^[25]. The decision function was obtained in accordance with optimization theory.

The evaluation indices of the SVM model include determination coefficient (R^2), average relative error (ARE), mean absolute error (MAE), and root-mean-square error ($RMSE$).

2.3.3 PSO algorithm

SVM offers advantages in model prediction. However, no specific theory on parameter selection (penalty parameter of C and kernel function parameter of σ) in SVM studies and training affects the prediction accuracy and efficiency. In this study, particle swarm optimization (PSO) was selected to optimize the parameters of the model. The algorithm found the optimal solution of space through iterative optimization in the solution space. The particles' speed (v) and location (x) were calculated and updated by tracking two target values (individual extremum and global optimal solution), as shown in Equations (3) and (4):

$$v_{ij}(t+1) = w_v \cdot v_{ij}(t) + c_1 \cdot r_1 \cdot [l_{ij}(t) - x_{ij}(t)] + c_2 \cdot r_2 \cdot [l_{gj}(t) - x_{ij}(t)] \quad (3)$$

$$x_{ij}(t+1) = x_{ij}(t) + v_{ij}(t+1) \quad (4)$$

where, w_v denotes the inertia weight that determines the impact of previous velocity; c_1 and c_2 represent learning factors; and r_1 and r_2 are independently uniformly distributed random variables with range $[0,1]$; i and j represent the number of particle and dimension, respectively; $l_{ij}(t)$ represents the individual extremum component in the j^{th} dimension; and $l_{gj}(t)$ is the global optimal solution in the t^{th} iteration. The algorithm will be terminated if the obtained optimal particle has met a certain objective function or has reached the maximum generation.

In the PSO algorithm, decreasing nonlinear processing is conducted on the important parameter inertia weight w_v to balance the global and local searching. Moreover, the learning factor (c_1 and c_2) affects the speed of particle optimization. However, the initial values of w_v , c_1 , and c_2 must be manually set. To avoid PSO from falling into the local optimum and to improve the convergence speed of late evolution and the performance

of the algorithm, improved inertia weight w_v was calculated by using Equation (5) and c_1 and c_2 by using Equation (6):

$$w_v = w_{\max} + \frac{(w_{\min} - w_{\max})(t_{\max} - t)}{t_{\max}} \quad (5)$$

$$\begin{cases} c_1 = c_{1,ini} + \frac{c_{1,fin} - c_{1,ini}}{t_{\max}} t \\ c_2 = c_{2,ini} + \frac{c_{2,fin} - c_{2,ini}}{t_{\max}} t \end{cases} \quad (6)$$

where, t_{\max} is the maximum generation; t is the current generation; and w_{\max} and w_{\min} represent the maximum and minimum inertia weights, respectively, i.e. $w \in (w_{\min}, w_{\max})$. $c_{1,ini}$ and $c_{1,fin}$ represent the original and final values of learning c_1 , respectively; and $c_{2,ini}$ and $c_{2,fin}$ represent the original and final values of learning c_2 , respectively.

3 Results and discussion

The environmental parameters in the greenhouse were automatically measured using the WSN system. The net photosynthetic rate of the tomato plants was obtained using the photosynthesis system. The net photosynthetic rate matched the environmental parameters on the basis of the comparison of the time series and conversion units.

3.1 ICA

Environmental information, including CO_2 concentration, light intensity, air temperature, air humidity, substrate temperature, and moisture, significantly influenced leaf photosynthesis and crop growth. Moreover, these parameters correlated with one another. The correlation among these environmental parameters was analyzed using SPSS. A significant correlation was found between air temperature and substrate temperature ($R=0.53$, $p<0.01$) as well as between air temperature and substrate moisture ($R=-0.32$, $p<0.01$). Hence, the input variables included redundant information, which affected the prediction speed and efficiency of SVM. The Fast ICA algorithm was used in extracting the independent component matrix to reduce redundancy and mine implicative information. Six dimensions of environmental parameters were included in this experiment. The number of ICs is $\in (2, 6)$ because the number of ICs is not more than the dimension number

of the environmental parameters. The ICs were used as input variables of the SVM-based prediction model to maximize the original information and improved the training speed, the number of ICs was increased gradually from 2 to 6 using the model input variables. The model performance is shown in Figure 3.

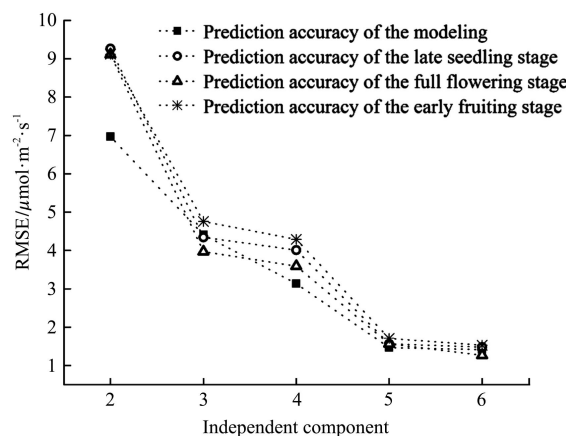


Figure 3 Prediction accuracy of the established model under varying IC numbers

Figure 3 shows that $RMSE$ gradually decreased as the number of ICs increased. This result indicates that ICs decomposed from raw information could not accurately express sample information when the number of ICs is small, whereas ICs contain the complete sample information when the number of ICs gradually increases. When the number of ICs was five, the $RMSE$ of the model fluctuated between 1.46 and 1.71. Therefore, the five dimensions of ICs were used as the input variables of the model.

3.2 Establishment of the photosynthesis prediction model

Data were collected at the late seedling, full flowering, and early fruiting stages of tomato plants during CO_2 enrichment period. The photosynthesis prediction model must be tested at the three growth stages because the photosynthetic rate of tomato leaves varies at these growth stages. The dataset was randomly divided into the training and testing groups. The training group was used to train the SVM, and the testing group was used to verify the effectiveness of the models. A total of 481 sample sets were collected in this experiment, of which 362 were assigned to the training group and 119 were assigned to the testing group. In the training group, 142 sample sets were selected from the late seedling stage,

113 from the full flowering stage, and 107 from the early fruiting stage. In the testing group, 47 sample sets were collected from the late seedling stage, 37 from the full flowering stage, and 35 from the early fruiting stage. PSO and its improved version were utilized to optimize and achieve the parameters (penalty parameter of C and kernel function parameter of σ) of SVM in the two prediction models. The other necessary parameters of the algorithm are provided in Table 1.

In the improved PSO-SVM model, the values of C and σ were 15.22 and 0.72, and the resulting performances R^2 , ARE , MAE , and $RMSE$ of the training group were 0.96, 0.33, 1.51, and 1.30, respectively. In the PSO-SVM model, the values of C and σ were 9.22 and 1.45, and the resulting average performances were 0.87, 0.54, 2.93, and 2.33, respectively. The testing

groups for the different growth stages were processed to verify the effectiveness of the established models. Figure 4 shows the comparison between the simulated and measured values obtained from testing using the original and improved PSO-SVM, respectively. In addition, Table 2 shows the comparison results.

Table 1 Values of the parameters involved in the algorithm

	Improved PSO	PSO
Searching range of C	(0.1, 1000)	(0.1, 1000)
Searching range of σ	(1, 1000)	(0.1, 1000)
Maximum generation	200	200
Particle population	20	20
Learning factor c_1 and c_2	—	1.5, 1.7
$c_{1,ini}$ and $c_{1,fini}$	3.5, 0.3	—
$c_{2,ini}$ and $c_{2,fini}$	0.5, 3.0	—
Inertia weight w	—	1
w_{max} and w_{min}	1.2, 0.1	—

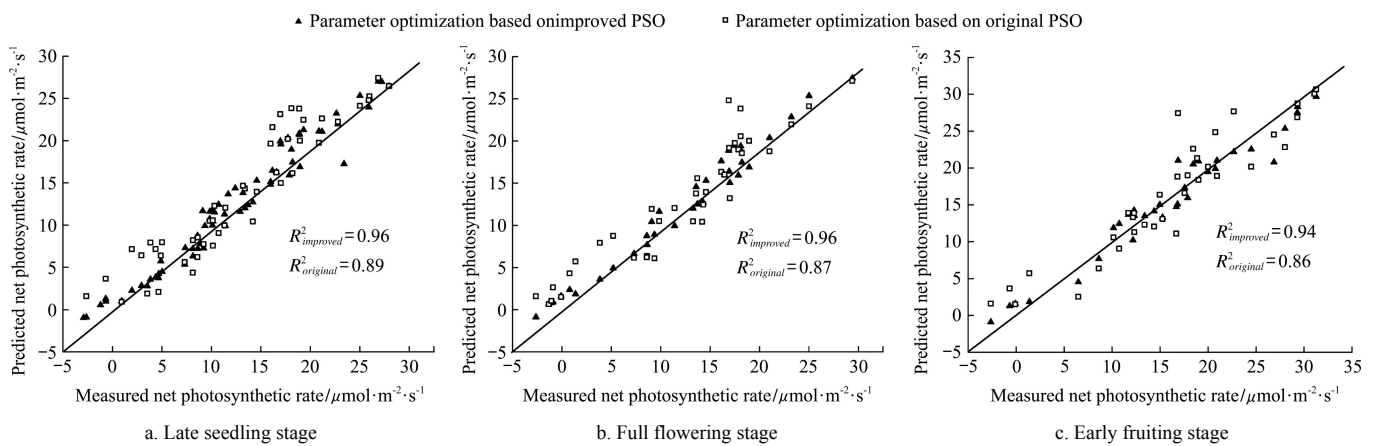


Figure 4 Prediction effects of the improved PSO-SVM and original PSO-SVM

Table 2 Evaluation indices of the two models for various growth stages

	Improved PSO-SVM			PSO-SVM		
	Late seedling stage	Full flowering stage	Early fruiting stage	Late seedling stage	Full flowering stage	Early fruiting stage
R^2	0.96	0.96	0.94	0.89	0.87	0.86
$ARE/\%$	11	9	12	31	33	29
$RMSE/\mu\text{mol}\cdot\text{m}^{-2}\cdot\text{s}^{-1}$	1.34	1.35	1.96	2.73	2.87	3.30
$MAE/\mu\text{mol}\cdot\text{m}^{-2}\cdot\text{s}^{-1}$	1.09	1.20	1.58	2.20	2.36	2.60

Table 2 shows that the R^2 of the values between the simulated and observed datasets for the three growth stages were 0.96, 0.96, and 0.94 with the improved PSO-SVM and 0.89, 0.87 and 0.86 with the original PSO-SVM. The results indicate that the improved PSO-SVM offers better performance in training and testing in terms of prediction accuracy and effects compared with the original PSO-SVM. This prediction model also showed high determination coefficient and

low error for the various growth stages, demonstrating that the improved PSO-SVM is an effective method in predicting photosynthetic rate at the entire growth stage of tomato.

3.3 Application of the photosynthesis prediction model in CO₂ concentration management

The light intensity, which considerably changes from morning to night, was difficult to control artificially in the greenhouse. However, this parameter significantly

affects the photosynthetic rate. Researches had shown that the photosynthetic rate of tomato plants decreases under low-intensity light^[26]. Moreover, photosynthesis is limited under CO₂ starvation during the midday when the light intensity is very high^[27,28]. Therefore, studies on the relationship between CO₂ concentration and photosynthetic rate are highly necessary for CO₂ enrichment under varying light intensities. Established photosynthesis prediction model showed that the maximum photosynthetic rate at varying light intensities can be obtained by changing the CO₂ concentration under certain environmental conditions at the three growth stages. The details are as follows.

3.3.1 Prediction effect at the late seedling stage

Figure 5 shows the relationship between CO₂ concentration and photosynthetic rate at the late seeding stage. Table 4 presents detailed information on data sets. The environmental parameters in the different growth stages were set as Table 3.

Figure 5 indicates that the maximum photosynthetic rate was achieved when the CO₂ concentration reached 1200 μmol/mol at 900 μmol/m²·s light intensity. Moreover, the CO₂ concentration corresponding to the maximum photosynthetic rate was the optimal CO₂ concentration. However, when the light intensities were 1200 and 600 μmol/m²·s, the prediction result showed no

obvious CO₂ saturation point. Table 4 shows the data used to generate Figure 5.

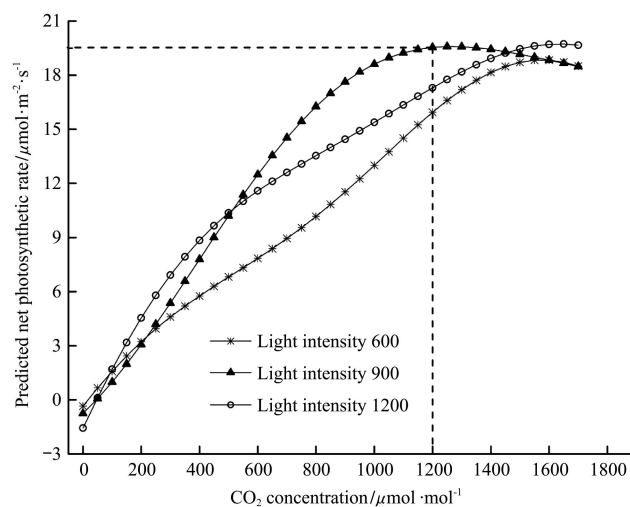


Figure 5 Relationship between CO₂ concentration and photosynthetic rate under varying light intensities at the late seedling stage

Table 3 Environmental variables in various growth stages

	Late seedling stage	Full flowering stage	Early fruiting stage
Air temperature/°C	32.74	33.30	31.47
Air humidity/%	30.38	34.12	38.25
Substrate temperature/°C	23.59	22.73	27.10
Substrate moisture/%	28.19	38.63	34.30
Light intensity/μmol·m ⁻² ·s ⁻¹	600, 900, 1200		
CO ₂ concentration /μmol·mol ⁻¹	0, 50, 100, 150, 200, 250, 300, 350, 400, 1500, 1550, 1600, 1650, 1700		

Note: CO₂ concentration changed from 0 to 1700 μmol/mol, and the interval was set to 50 μmol/mol.

Table 4 Photosynthetic rate prediction values of improved PSO-SVM model in the late seedling stage

Light intensity /μmol·m ⁻² ·s ⁻¹	CO ₂ concentration gradient/μmol·mol ⁻¹																	
	0	50	100	150	200	250	300	350	400	450	500	550	600	650	700	750	800	850
600	-0.35	0.65	1.58	2.43	3.22	3.93	4.59	5.19	5.76	6.29	6.81	7.33	7.85	8.38	8.95	9.54	10.17	10.83
900	-0.76	0.07	0.98	1.98	3.06	4.19	5.37	6.57	7.79	9.00	10.20	11.37	12.49	13.54	14.53	15.44	16.27	17.00
1200	-1.57	0.11	1.69	3.17	4.54	5.79	6.92	7.93	8.84	9.65	10.37	11.01	11.59	12.12	12.61	13.08	13.54	13.99
	900	950	1000	1050	1100	1150	1200	1250	1300	1350	1400	1450	1500	1550	1600	1650	1700	
600	11.53	12.26	13.00	13.76	14.51	15.24	15.94	16.60	17.20	17.72	18.15	18.49	18.72	18.83	18.84	18.72	18.50	
900	17.63	18.17	18.62	18.97	19.24	19.43	19.54	19.59	19.58	19.53	19.43	19.31	19.16	19.00	18.83	18.66	18.48	
1200	14.45	14.91	15.38	15.86	16.34	16.83	17.30	17.76	18.19	18.58	18.93	19.22	19.46	19.62	19.71	19.73	19.67	

3.3.2 Prediction effect at the full flowering stage

Figure 6 shows the prediction relationship curve at the full flowering stage, and the detail information is shown in Table 5. The parameters were settings as shown in Table 3. Figure 6 also shows that the photosynthetic rate gradually became saturated with increasing CO₂ concentration. In addition, the maximum photosynthetic rates were 17.57 μmol/m²·s, 23.17 μmol/m²·s, and

25.51 μmol/m²·s under light intensities of 600 μmol/m²·s, 900 μmol/m²·s, and 1200 μmol/m²·s, respectively. When the light intensity changed from 600 μmol/m²·s to 1200 μmol/m²·s, the photosynthetic rate increased under the same CO₂ concentration, and the CO₂ concentration saturation point shifted backward. This phenomenon shows that the photosynthetic ability of tomato leaf was strong in this period. Table 5 shows the data used to

generate Figure 6.

3.3.3 Prediction effect at the early fruiting stage

Figure 7 shows the prediction relationship curve at the early fruiting stage, and the detail information is shown in Table 6. The environment parameters are shown in Table 3. Figure 7 shows that the photosynthetic rate was lower at 1200 $\mu\text{mol}/\text{m}^2\cdot\text{s}$ than at 900 $\mu\text{mol}/\text{m}^2\cdot\text{s}$ light intensity. This result may be ascribed to the aging of the

tomato leaf and the reduction in light saturation point. The maximum photosynthetic rate was achieved when CO_2 concentration reached 1100 $\mu\text{mol}/\text{mol}$ at a light intensity of 900 $\mu\text{mol}/\text{m}^2\cdot\text{s}$. The photosynthetic rate did not reach its saturation point when the light intensity was only 600 $\mu\text{mol}/\text{m}^2\cdot\text{s}$. Table 6 shows the data used to generate Figure 7.

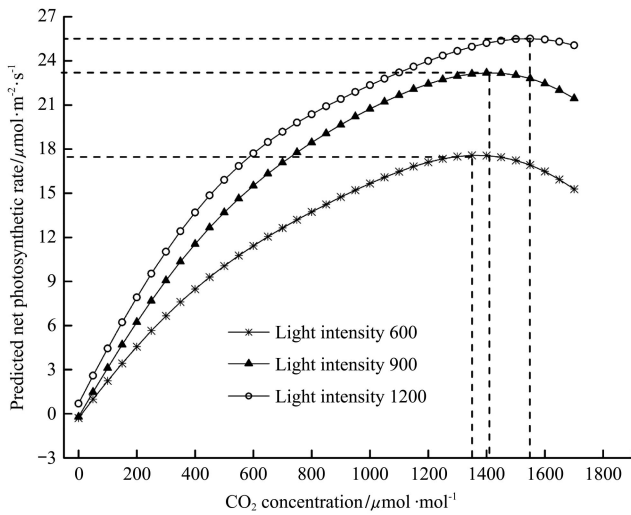


Figure 6 Relationship between CO_2 concentration and photosynthetic rate under varying light intensities at the full flowering stage

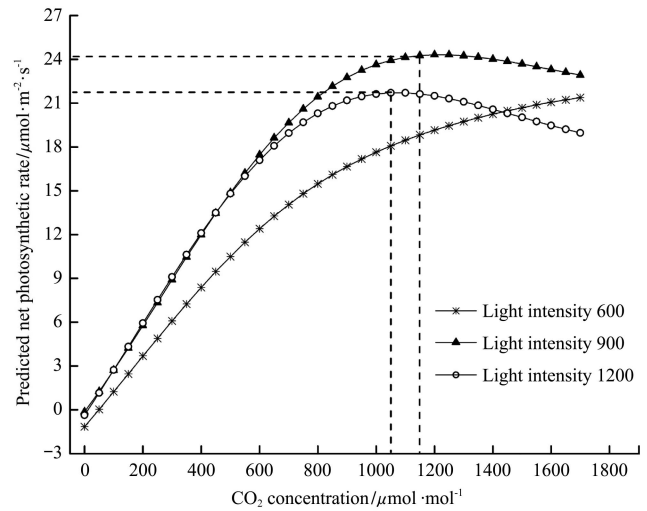


Figure 7 Relationship between CO_2 concentration and photosynthetic rate under varying light intensities at the early fruiting stage

Table 5 Photosynthetic rate prediction values of improved PSO-SVM model in the full flowering stage

Light intensity $\mu\text{mol}\cdot\text{m}^{-2}\cdot\text{s}^{-1}$	CO_2 concentration gradient/ $\mu\text{mol}\cdot\text{mol}^{-1}$																	
	0	50	100	150	200	250	300	350	400	450	500	550	600	650	700	750	800	850
600	-0.29	0.99	2.24	3.43	4.57	5.65	6.66	7.60	8.48	9.30	10.06	10.76	11.42	12.04	12.63	13.19	13.73	14.24
900	-0.21	1.47	3.11	4.70	6.23	7.69	9.06	10.35	11.55	12.66	13.69	14.64	15.51	16.33	17.08	17.79	18.45	19.07
1200	0.70	2.59	4.44	6.22	7.92	9.53	11.03	12.42	13.69	14.85	15.91	16.86	17.71	18.48	19.17	19.80	20.37	20.91
	900	950	1000	1050	1100	1150	1200	1250	1300	1350	1400	1450	1501	1550	1600	1650	1701	
600	14.74	15.21	15.66	16.08	16.47	16.82	17.11	17.34	17.50	17.58	17.56	17.45	17.24	16.91	16.48	15.93	15.27	
900	19.66	20.21	20.73	21.22	21.67	22.08	22.43	22.73	22.96	23.11	23.18	23.15	23.03	22.80	22.46	22.00	21.44	
1200	21.41	21.89	22.34	22.78	23.21	23.61	24.00	24.36	24.68	24.97	25.20	25.38	25.48	25.51	25.46	25.31	25.06	

Table 6 Photosynthetic rate prediction values of improved PSO-SVM model in the early fruiting stage

Light intensity $\mu\text{mol}\cdot\text{m}^{-2}\cdot\text{s}^{-1}$	CO_2 concentration gradient/ $\mu\text{mol}\cdot\text{mol}^{-1}$																	
	0	50	100	150	200	250	300	350	400	450	500	550	600	650	700	750	800	850
600	-1.15	0.03	1.24	2.46	3.68	4.89	6.09	7.25	8.38	9.46	10.50	11.48	12.40	13.26	14.06	14.80	15.48	16.10
900	-0.14	1.25	2.71	4.23	5.77	7.34	8.91	10.47	11.99	13.46	14.88	16.21	17.46	18.62	19.67	20.61	21.44	22.15
1200	-0.36	1.16	2.73	4.32	5.93	7.53	9.10	10.63	12.10	13.49	14.80	16.00	17.10	18.08	18.95	19.69	20.30	20.80
	900	950	1000	1050	1100	1150	1200	1250	1300	1350	1400	1450	1500	1550	1600	1650	1700	
600	16.66	17.18	17.65	18.08	18.47	18.82	19.15	19.45	19.74	20.00	20.24	20.47	20.69	20.89	21.07	21.23	21.37	
900	22.75	23.25	23.64	23.94	24.14	24.26	24.32	24.31	24.25	24.15	24.01	23.86	23.68	23.50	23.31	23.12	22.93	
1200	21.18	21.46	21.63	21.71	21.70	21.63	21.50	21.32	21.09	20.85	20.58	20.30	20.02	19.74	19.47	19.21	18.97	

In summary, the photosynthesis prediction model can basically predict the photosynthetic rate at the entire growth stage of tomato. Under specified conditions, the model can determine the relationship between CO₂ concentration and photosynthetic rate and make the appropriate application of CO₂ enrichment possible to ensure the enhancement of plant growth.

Furthermore, the experimental results only reflected the short-term response of the plant to CO₂ concentration in daylight. Long-term studies are thus necessary to evaluate whether or not CO₂ enrichment consistently promotes photosynthesis. Other environmental variables and physiological parameters, such as air temperature, substrate moisture, chlorophyll content, and stomatal conductance, also exerted important effects on photosynthesis in tomato plants. Further experiments are needed to elucidate the reciprocal interaction influence of CO₂ enrichment and other key factors.

4 Conclusions

This study determined and analyzed the photosynthetic rate of tomato plants at three growth stages. An environment monitoring system was built to measure environmental information automatically. The photosynthetic rate was obtained using the LI-6400XT portable photosynthesis system. The photosynthesis prediction models of the entire growth stage of tomato were established using PSO-SVM and its improved version. The conclusions are as follows:

1) Environmental parameters were processed using the ICA method to reduce redundancy and to identify the implicative information of input variables. Five independent input variables that can improve prediction accuracy and efficiency were obtained for the model.

2) An improved PSO algorithm was applied to optimize the SVM parameters, which improved the original PSO from the aspect of nonlinear processing of learning factors and inertia weight. The improved PSO-SVM model was evaluated using the testing group with addition samples in different growth stages, and then compared this model with the PSO-SVM model. The simulation results showed that the improved PSO-SVM method can achieve high prediction accuracy at the three

growth stages and that the model can adequately predict photosynthetic rate.

3) The relationship between CO₂ concentration and photosynthetic rate was analyzed to ensure that a proper amount of CO₂ is provided to the tomato plants under varying light intensities at the three growth stages. The photosynthetic rate significantly increased and then peaked with increasing CO₂ concentration. When the light intensity changed from 600 $\mu\text{mol}/\text{m}^2\cdot\text{s}$ to 1200 $\mu\text{mol}/\text{m}^2\cdot\text{s}$, the relationship between CO₂ and photosynthetic rate was changed, the photosynthetic rate changed from low to high, and the CO₂ saturation points shifted. Therefore, the model is useful in CO₂ enrichment under greenhouse conditions.

Acknowledgements

This work was supported by the National Key Research and Development Program (Grant No. 2016YFD0200602) and National Natural Science Fund (Grant No. 31271619).

[References]

- [1] Ryu D K, Ryu M J, Chung S O, Hur S O, Hong S J, Sung J H, et al. Variability of soil water content, temperature, and electrical conductivity in strawberry and tomato greenhouses in winter. *J. Biosyst. Eng.*, 2014; 37: 39–46.
- [2] Guo W, Cheng H, Li R, Li J, Zhang H. Greenhouse monitoring system based on wireless sensor networks. *Transactions of the CSAM*, 2010; 41(7): 181–185. (in Chinese)
- [3] Li Y H, Ji G F, Han J Y. Application of the wireless sensor network in environment monitoring system of greenhouse. *Instrument and Meter for Automation*, 2010; 31(10): 61–64. (in Chinese)
- [4] Mancuso M, Bustaffa F. A wireless sensors network for monitoring environmental variables in a tomato greenhouse. *IEEE International Workshop on Factory Communication Systems*, 2006; pp.107–110.
- [5] Srbinovska M, Gavrovski C, Dimcev V, Krkoleva A, Borozan V. Environmental parameters monitoring in precision agriculture using wireless sensor networks. *Journal of Cleaner Production*, 2015; 88: 297–307.
- [6] Hwang J, Shin C, Yoe H. A wireless sensor network-based ubiquitous paprika growth management system. *Sensors*, 2010; 10(12): 11566–11589.
- [7] Prior S A, Brett Runion G, Rogers H H, Allen Torbert H,

- Wayne Reeves D. Elevated atmospheric CO₂ effects on biomass production and soil carbon in conventional and conservation cropping systems. *Global Change Biology*, 2005; 11(4): 657–665.
- [8] Poorter H, Navas M L. Plant growth and competition at elevated CO₂: on winners, losers and functional groups. *New Phytologist*, 2003; 157(2): 175–198.
- [9] Kimball B A, Kobayashi K, Bindi M. Responses of agricultural crops to free-air CO₂ enrichment. *Advances in Agronomy*, 2002; 77: 293–368.
- [10] Dehshiri A, Modarres-Sanavy S A M, Mahdavi B. Amelioration of salinity on photosynthesis and some characteristics of three rapeseed (*Brassica napus*) cultivars under increased concentrations of carbon dioxide. *Archives of Agronomy and Soil Science*, 2015; 61(10): 1423–1438.
- [11] Wang W Z, Zhang M, Liu C H, Li M Z, Liu G. Real-time monitoring of environmental information and modeling of the photosynthetic rate of tomato plants under greenhouse conditions. *Applied Engineering in Agriculture*, 2013; 29(5): 783–792.
- [12] Zhang J, Wang S. Simulation of the canopy photosynthesis model of greenhouse tomato. *Procedia Engineering*, 2011; 16: 632–639. (in Chinese)
- [13] Hu J, He D, Ren J, Liu X, Liang Y, Dai J, et al. Optimal regulation model of tomato seedlings' photosynthesis based on genetic algorithm. *Transactions of the CSAE*, 2014; 30(17): 220–227. (in Chinese)
- [14] Wang D, Wang M, Qiao X. Support vector machines regression and modeling of greenhouse environment. *Computers and Electronics in Agriculture*, 2009; 66(1): 46–52.
- [15] Zai S, Wen J, Guo D, Han Q, Deng Z, Sun H, et al. Determination of leaf area of sweet pepper based on support vector machine model and image processing. *Transactions of the CSAE*, 2011; 27(3): 237–241. (in Chinese)
- [16] Zhang Y, Zheng L, Li M, Deng X, Ji R. Predicting apple sugar content based on spectral characteristics of apple tree leaf in different phenological phases. *Computers and Electronics in Agriculture*, 2015; 112: 20–27.
- [17] Liu B, Hou D, Huang P, Liu B, Tang H, Zhang W et al. An improved PSO-SVM model for online recognition defects in eddy current testing. *Nondestructive Testing & Evaluation*, 2013, 28(4): 367–385.
- [18] Kennedy J, Eberhart R. Particle swarm optimization. *Proceedings of IEEE International Conference on Neural Networks*, 1995: 1942–1948.
- [19] Xu X, Guan X P, Hua C C. Modeling of blast furnace temperature based on improved particle swarm optimizer and support vector machine. Hebei Province, Yanshan University, 2015. (in Chinese)
- [20] Xu S, Zhu X, Li C, Ye Q. Effects of CO₂ enrichment on photosynthesis and growth in *Gerbera jamesonii*. *Scientia Horticulturae*, 2014; 177: 77–84.
- [21] Manual LI-6400XT OPEN6.1. Lincoln, NE, USA: LI-COR Inc.
- [22] Liu N J, Shi B L, Zhao L, Qing Z S, Ji B P, Zhou F. Analysis of feature signals of electronic nose in honey nectar detection based on independent components analysis combined with genetic algorithm. *Transactions of the CSAE*, 2015; 31(Supp.1): 315–324. (in Chinese)
- [23] Sun T, Xu W, Hu T, Liu M H. Determination of soluble solids content in Nanfeng Mandarin by Vis/NIR spectroscopy and UVE-ICA-LS-SVM. *Spectroscopy and Spectral Analysis*, 2013; 33(12): 3235–3239. (in Chinese)
- [24] Hyvärinen A, Oja E. Independent component analysis: algorithms and applications. *Neural Networks*, 2000; 13(4): 411–430.
- [25] Lin S, Liu Z. Parameter selection in SVM with RBF kernel function. *Journal-Zhejiang University of Technology*, 2007; 35(2): 163–167. (in Chinese)
- [26] Hu W, Yan X, Yuan L, Yang Q, Wu Z. The role of light intensity in the recovery of photosynthesis in the tomato leaves after chilling under low light. *Bulletin of Botanical Research*, 2011; 31(2): 164–168. (in Chinese)
- [27] Thongbai P, Kozai T, Ohyama K. CO₂ and air circulation effects on photosynthesis and transpiration of tomato seedlings. *Scientia Horticulturae*, 2010; 126(3): 338–344.
- [28] Sánchez-Guerrero M C, Lorenzo P, Medrano E, Castilla N, Soriano T, Baille A. Effect of variable CO₂ enrichment on greenhouse production in mild winter climates. *Agricultural and Forest Meteorology*, 2005; 132(3): 244–252.